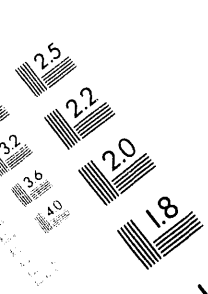

Association for Information and Image Management

1100 Wayne Avenue, Suite 1100
Silver Spring, Maryland 20910

301/587-8202

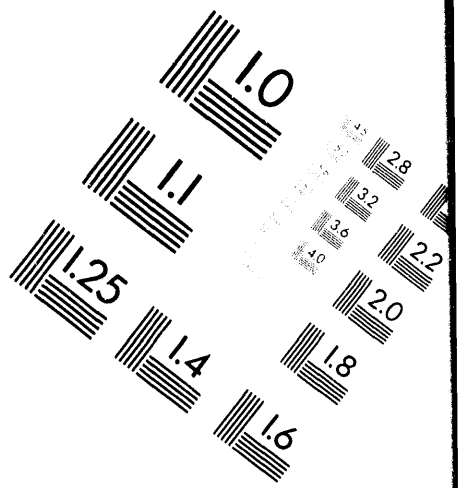

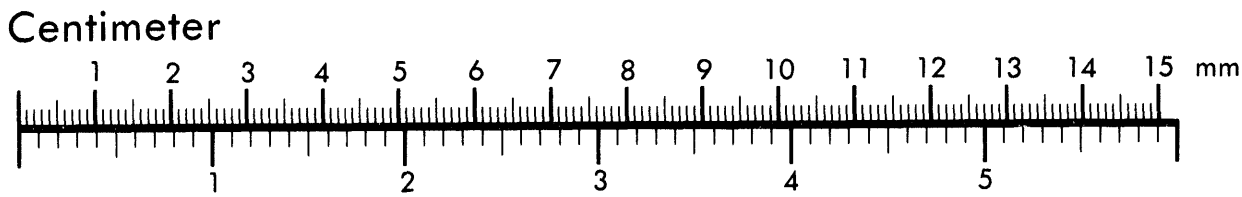

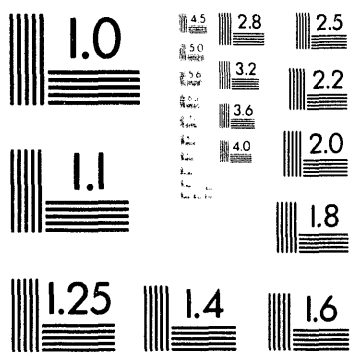

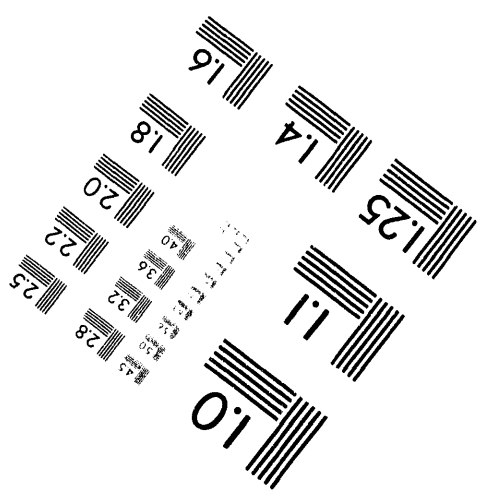

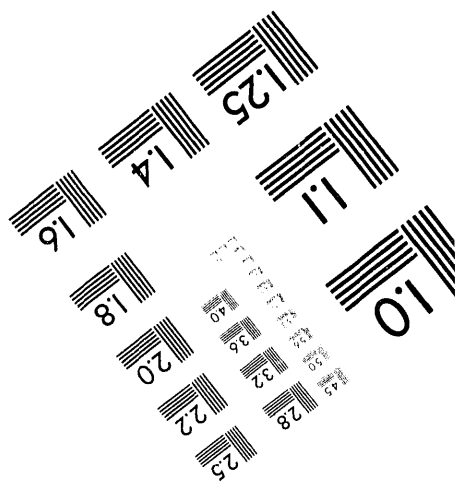

MANUFACTURED TO AIIM STANDARDS
BY APPLIED IMAGE, INC.

1 of 1

Conf-9403116--1

LA-UR- 94-1455

Title: MAGNETOTAIL DYNAMICS: MHD SIMULATIONS OF DRIVEN AND SPONTANEOUS DYNAMIC CHANGES

Author(s): J. Birn, NIS-1, Los Alamos, NM
K. Schindler, Theoretische Physik IV, Bochum, University
M. Hesse, Electrodynamics Branch, NASA, Greenbelt, MD

Submitted to: ICS2 Proceedings
Fairbanks, Alaska
March 7-11, 1994

DISCLAIMER

This report was prepared as an account of work sponsored by an agency of the United States Government. Neither the United States Government nor any agency thereof, nor any of their employees, makes any warranty, express or implied, or assumes any legal liability or responsibility for the accuracy, completeness, or usefulness of any information, apparatus, product, or process disclosed, or represents that its use would not infringe privately owned rights. Reference herein to any specific commercial product, process, or service by trade name, trademark, manufacturer, or otherwise does not necessarily constitute or imply its endorsement, recommendation, or favoring by the United States Government or any agency thereof. The views and opinions of authors expressed herein do not necessarily state or reflect those of the United States Government or any agency thereof.

MASTER

Los Alamos
NATIONAL LABORATORY

Los Alamos National Laboratory, an affirmative action/equal opportunity employer, is operated by the University of California for the U.S. Department of Energy under contract W-7405-ENG-36. By acceptance of this article, the publisher recognizes that the U.S. Government retains a nonexclusive, royalty-free license to publish or reproduce the published form of this contribution, or to allow others to do so, for U.S. Government purposes. The Los Alamos National Laboratory requests that the publisher identify this article as work performed under the auspices of the U.S. Department of Energy.

Form No. 836 R5
ST 2629 10/91

DISTRIBUTION OF THIS DOCUMENT IS UNLIMITED

MAGNETOTAIL DYNAMICS: MHD SIMULATIONS OF DRIVEN AND SPONTANEOUS DYNAMIC CHANGES

J. Birn

Space and Atmospheric Sciences Group, Los Alamos National Laboratory, Los Alamos, New Mexico 87545

K. Schindler

Theoretische Physik IV, Ruhr-Universität, D-44780 Bochum, Germany

M. Hesse

Electrodynamics Branch, NASA, Goddard Space Flight Center, Greenbelt, Maryland 20771

Abstract

The dynamic evolution of the magnetotail during growth phase and expansion phase of a substorm is studied through three-dimensional time-dependent MHD simulations. To model growth phase effects, an external electric field with an equatorward inflow is applied at the boundaries over a finite time period. This leads to the formation of a thin current sheet with greatly enhanced current density in the near tail, embedded in the wider plasma/current sheet, which becomes diminished in strength. A faster, spontaneous current sheet formation occurs when entropy conservation is released in an isobaric model, while the ideal MHD constraint persists. This may be a suitable model for the late, explosive part of the growth phase. The transition to the substorm expansive phase is modeled by an increase in anomalous resistivity, using either uniform resistivity or a current density dependent resistivity which is turned on when the current density exceeds a certain threshold. In both cases the violation of ideal MHD leads to resistive instability and the formation of a near-Earth neutral line, fast flow, and plasmoid ejection, together with the dipolarization and current reduction in the region further earthward. The spontaneous increase in total region 1 type field-aligned currents associated with the disruptions of the thin current sheets is less significant than that found in earlier simulations of the disruption of a wider current sheet, whereas the driven increase in the region 1 type current is substantial. The results demonstrate that the same dynamic process which appears spontaneous in the behavior of some quantities might be interpreted as entirely driven from the observation of others.

1. Introduction

One of the most significant recent results concerning substorm onset conditions and magnetotail dynamics is the formation of a thin current sheet in the near tail in the late substorm growth phase, well documented from observations at distances of about 8 to 15 R_E [e.g., McPherron et al., 1987; Mitchell et al., 1990;

Pulkkinen et al., 1992; Ohtani et al., 1992; Lui et al. 1992; Sergeev et al., 1993]. This near-Earth current sheet thins to a scale length in the north-south direction (current sheet half-thickness) of about 1000-2000 km, which is only about 1/10 of the tail current sheet half-thickness during quiet times. In contrast to the thinning observed at or after substorm onset at larger distances [e.g., Hones et al., 1984; Sauvaud et al., 1984], this current sheet apparently forms inside the wider plasma sheet, which seems to persist during the growth phase [Sergeev et al., 1993]. The purpose of the present paper is to investigate the formation of this current sheet and its influence on the subsequent dynamic evolution of the magnetotail in the framework of large-scale fluid theory, using three-dimensional MHD simulations. A parallel study [Hesse et al., this issue] focuses on the effects of the near tail geometry with its transition from the taillike to a dipolar field on the dynamic evolution, assuming that a thin current sheet is already established in the near tail.

The present model is based on the generally accepted substorm scenario in which the growth phase in the magnetotail is the consequence of magnetic reconnection at the frontside of the magnetosphere with subsequent transport of magnetic flux and energy into the tail, associated with an increase in plasma convection, electric fields, and currents. We will show that a thin current sheet forms as the consequence of an electric field applied at the boundaries of the tail section considered. In another model a more rapid formation may occur more spontaneously as the consequence of a sudden release of entropy conservation on convecting magnetic flux tubes, which might be relevant for the observed final "explosive" part of the growth phase [Ohtani et al., 1992]. The further evolution is assumed to be the consequence of nonideal effects, that is, a violation of the frozen-in field constraint of ideal MHD, which is modeled by an increase in (anomalous) resistivity. The resistivity models pertain most closely to the expected effects of a current-driven micro-instability, such as the cross-field instability suggested by Lui et al. [1991]. However, since nonideal effects are important only in a localized region, we expect that the global dynamic changes will be similar when the local breakdown of ideal MHD is caused by other mechanisms, such as ion-tearing instability [Schindler, 1973].

2. Numerical Model

The initial state is a realistic three-dimensional equilibrium model of the magnetotail developed by Birn [1987], which was used in several previous investigations [e.g., Birn and Hesse, 1991]. It is illustrated in Figure 1 in the form of a magnetic flux surface emanating from an assumed circular cross section at its near-Earth end. It includes flaring of the tail in y and z and an increase in plasma sheet thickness from midnight toward the flanks by a factor of about 2 and a somewhat weaker increase downtail. The length units in Figure 1 are scaled by the current sheet half-thickness L_z at y=0 and the near-Earth end x=0 of the tail section considered. Here and in the following we use dimensionless units, normalized at the near-Earth boundary by the initial current sheet half-thickness L_Z=12000km, a lobe magnetic field strength B_L=40nT, a characteristic Alfvén speed v_A=1000km/s, defined by the characteristic lobe magnetic field strength and the plasma sheet densiy, and suitable combinations of these quantities. This yields, for instance, a time scale $t_A=L_z/v_A$=12s.

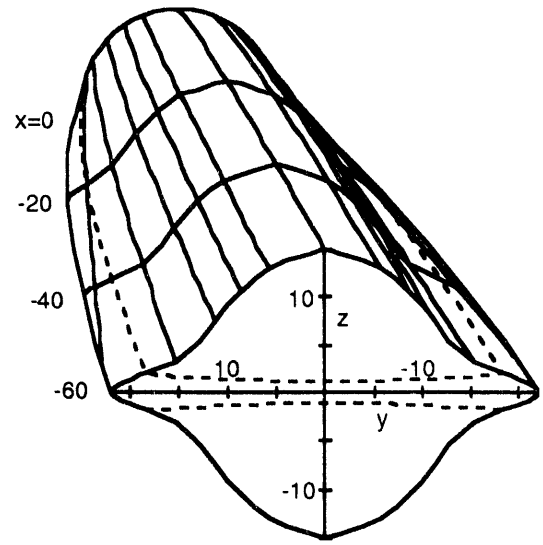

Fig. 1: Initial tail configuration. Magnetic flux surface originating from a circle of 10 units radius (about 20 R_E) at the near-Earth boundary x=0. The dashed line represents the plasma/current sheet thickness.

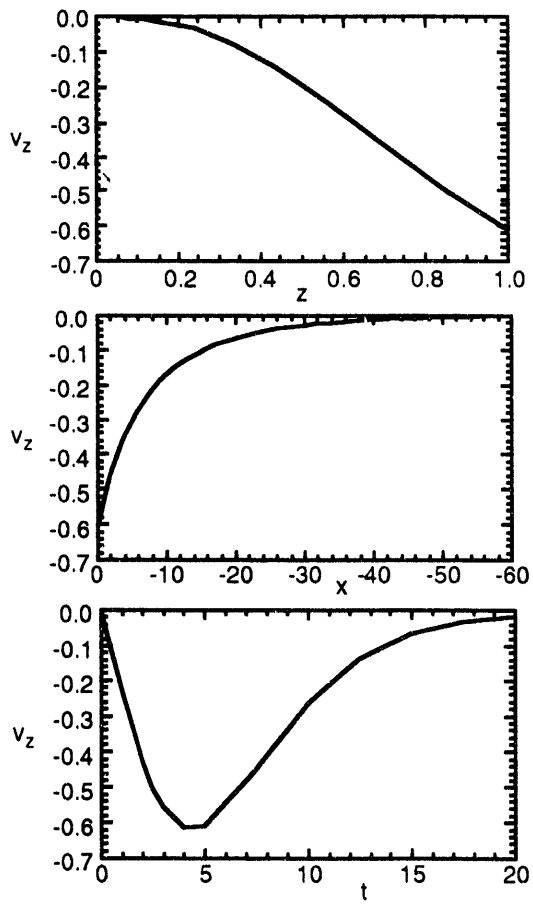

Fig. 2: Inflow speed v_z at the boundaries x=0 (top) and z=10 (center), and maximum speed as a function of time (bottom) for t_c=5.

The driving boundary conditions, which consist of an inflow in the z direction toward the equatorial plane, are shown in Fig. 2 by the variation of v_z at the boundary with x, z, and time. The inflow speed is maximal at the high-latitude near-Earth boundary at midnight and decreases toward the flanks (following a cosine law in y) and with distance along the tail. It also decreases equatorward, consistent with the decay of a similar linear perturbation of a plane current sheet investigated analytically [Schindler and Birn, 1993]. The inflow speed also varies with time, first increasing linearly and later decaying after some maximum is reached at a characteristic time scale t_c (t_c=5 in Fig. 2).

The code consists of an explicit finite difference scheme, which solves the time-dependent resistive MHD equations; it has been described earlier in more detail [e.g., Birn and Hesse, 1991]. Whereas v_z is prescribed at the near-Earth and high latitude boundaries, as mentioned above, the other velocity components are set to zero except at the distant boundary in x, where a free outflow condition is assumed. Neumann boundary conditions ($\partial/\partial n=0$) are imposed on density, pressure, and the tangential magnetic field components, while the normal magnetic field is held fixed (except for the near-Earth boundary, where B_x is calculated from consistency with $\nabla\bullet\mathbf{B}=0$. Symmetry conditions are used at z=0 and y=0. The MHD equations are integrated in a rectangular box $0\geq x\geq -60$, $0\leq y\leq 10$, $0\leq z\leq 10$.

Two different resistivity models are used, (a) constant resistivity $\eta=\eta_0$, corresponding to a Lundquist number (magnetic Reynolds number) $S=1/\eta_0$, and (b) current dependent resistivity given by

$$\eta=\eta_0 (j - j_o)^2 \quad \text{for } j > j_o$$
$$\eta=0 \quad \text{for } j < j_o$$

3. Current Sheet Formation

The formation of a thin current sheet in the near-Earth tail region as a consequence of the imposed boundary electric field is demonstrated in Figures 3 and 4. The characteristic time scale of the boundary perturbation is t_c=5, and η=0 is assumed for t<100. Fig. 3 shows the variation of B_z (top panel) and j_y (bottom panel) along the x axis and Fig. 4 the corresponding variation of j_y (top) and B_x (bottom) with z at x=-7.5, where j_y assumes its maximum. Various times are indicated in the figures. Note that t>100 corresponds to a resistive dynamic phase to be discussed in section 4. Here we concentrate on the effects of the driven phase t<100. While the boundary perturbations have subsided at about t=20, the new equilibrium with the thin current sheet is established at about t=50, although some long period (about 100 Alfvén times) fluctuations of the peak current density still occur at later times. Figures 3 and 4 clearly demonstrate the reduction of B_z and the significant increase of j_y by a factor of about 5, while the lobe magnetic field strength increases only by ~25% at this location. The strong current is concentrated in a sheet with a thickness of less than 1/5 of the original current sheet. Fig. 4 also shows that the original wide current sheet persists, although reduced in strength by ~50%; the thin current sheet contains 70-80% of the total enhanced curent. Fig. 3 shows that the thinning and current sheet formation affect a region of ~10 units (~20R_E) in x. The y extent, not shown here, is similar.

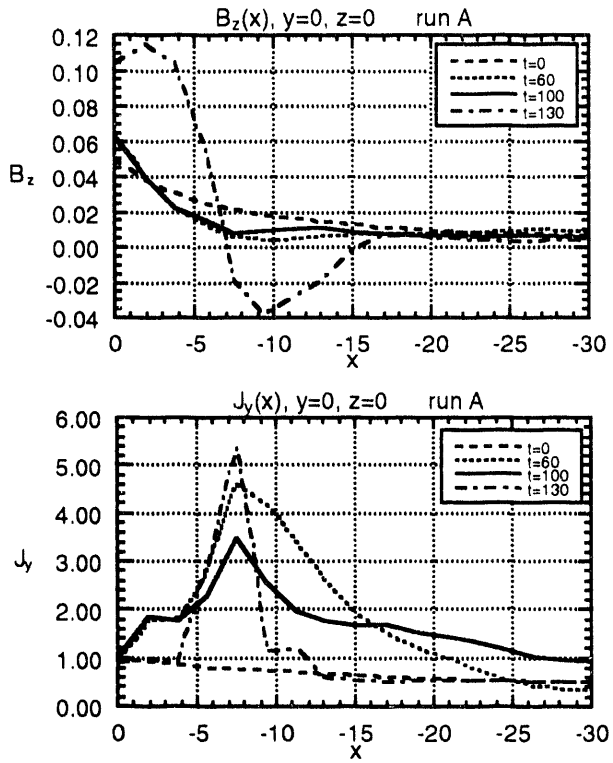

Fig. 3: Variation of B_z (top) and j_y (bottom) along the x axis for run A, modeling externally driven current sheet formation (t<100) and subsequent resisitive instability (t>100).

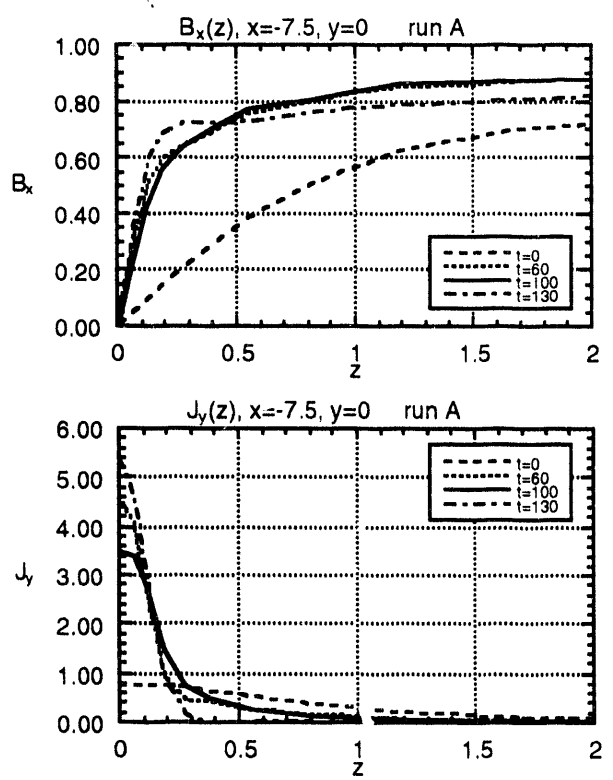

Fig. 4: Variation of B_z (top) and j_y (bottom) with z at x=-7.5, y=0 for run A.

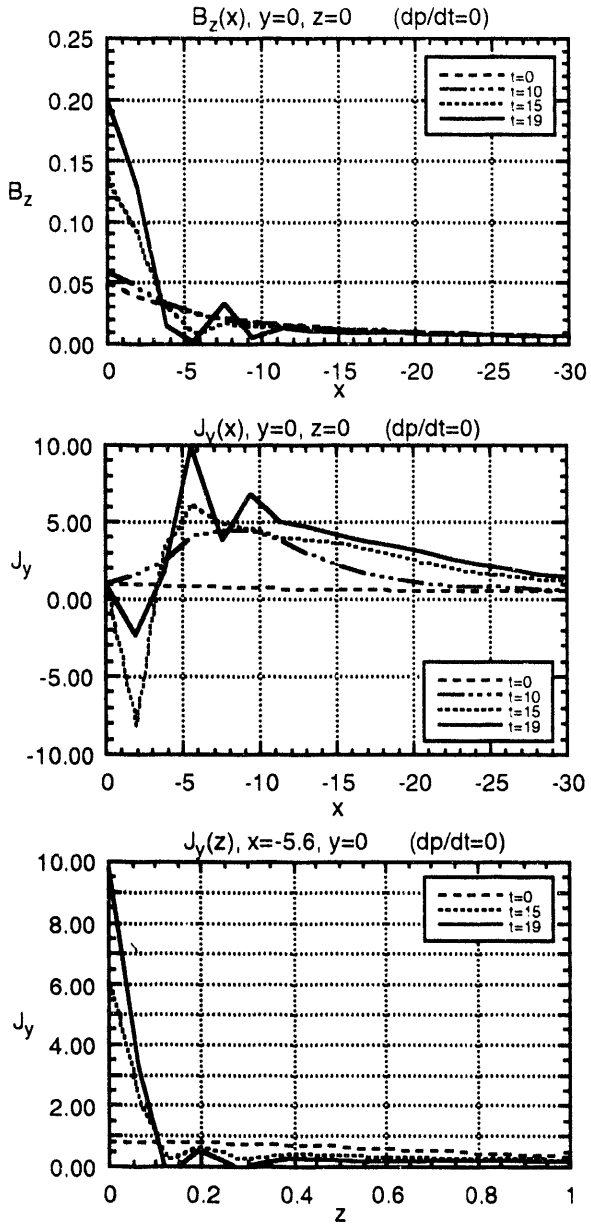

Fig. 5: Variation of B_z (top) and j_y (center) along the x axis and of j_y as a function of z at x=-5.6 (bottom) for spontaneous current sheet formation in an isobaric dynamic model.

The current sheet formation demonstrated by Figures 3 and 4 can be considered as a directly driven process, although the time scale of the evolution depends on the external time scale in a nonlinear way. For the chosen external time scale t_c of only 5 Alfvén times (~1 minute) it takes about 50 time units (~10 min) to achieve the new equilibrium with the thin current sheet. This time represents an internal adjustment time, independent of the external time scale t_c. When the driving time scale t_c is larger than the internal adjustment time, the internal changes are essentially quasi-static and roughly proportional to the external perturbations and the evolution can be considered as directly driven in a stricter sense.

Current sheet formation need not be a driven process as modeled above. In fact, observations [Ohtani et al., 1992] suggest that the late growth phase assumes an explosive character, which one might associate with some instability. Analytical and numerical studies by Birn et al. [1994] have shown that such an instability indeed might exist in an isobaric dynamic tail model with dp/dt=0, in which the ideal MHD field constraint is maintained, however, the conservation of entropy on convecting magnetic flux tubes becomes violated. This might be accomplished by particle or energy exchange with the ionosphere [Erickson and Heinemann, 1992] or through a nonadiabatic process in the tail [Birn et al., 1994]. Here we extend the Birn et al. simulations to three-dimensional configurations. Fig. 5 shows the variations of B_z (top) and j_y (center) along the x axis and the variations of j_y with z at x=-5.6 (bottom) for different times indicated in the figures. These figures show a similar current concentration and reduction of B_z as the driven case (Figures 3 and 4). However, the characteristic time scale for the formation is much shorter, only ~10 Alfvén times (~2 min).

4. Current Disruption

The strong increase of the current density associated with the formation of the thin current sheet in the near tail as well as the decrease of B_z in association with the small current sheet width can possibly trigger the onset of an instability [e.g., Schindler, 1973]. A small-scale current driven instability might generate anomalous resistivity [Lui et al., 1991] and hence lead to a resistive tearing mode or a collisionless tearing mode might be initiated directly. Here we will model the onset of instability through an onset of resistivity. In run A we take a late result (at t=100) of the driven process presented in the previous section and impose finite resistivity η=1/200, which is assumed constant and uniform, for simplicity. In run B we use the current density dependent resistivity model (b), defined in section 2, with η_o=1/200 and j_o=4, in which resistivity is turned on only if the current density exceeds a threshold of four times the initial maximum current density. For the external driving a more realistic, longer time scale t_c of 75 Alfvén times (~15 min) is used, associated with a maximum inflow speed of 0.07 (70 km/s). As a consequence the driving still continues while the instability sets in.

Some results of run A are already included in Figures 3 and 4 (for t>100). They demonstrate the dipolarization (increase in B_z) in the near tail, following the stretching (reduction in B_z) in the driven phase (t<100), and, further tailward, the southward turning of B_z, implying neutral line and plasmoid formation. The current density shows a further increase after t=100 in the vicinity of the near-Earth neutral line, however, a decrease

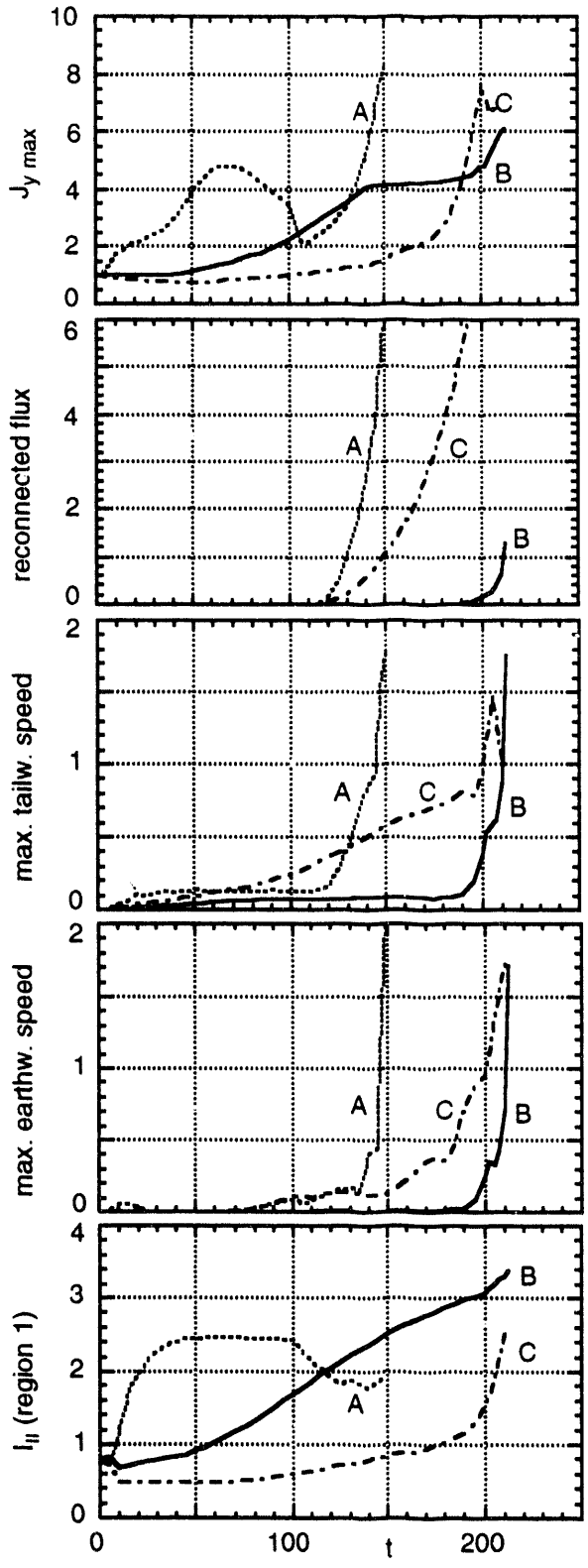

Fig. 6: Temporal variation of characteristic quantities. Run A: driven formation of a thin current sheet (η=0) and subsequent disruption (η=0.005) for t>100; run B: driven formation of a thin current sheet with $\eta=\eta(j)$; run C: disruption of a thick current sheet, η=0.005.

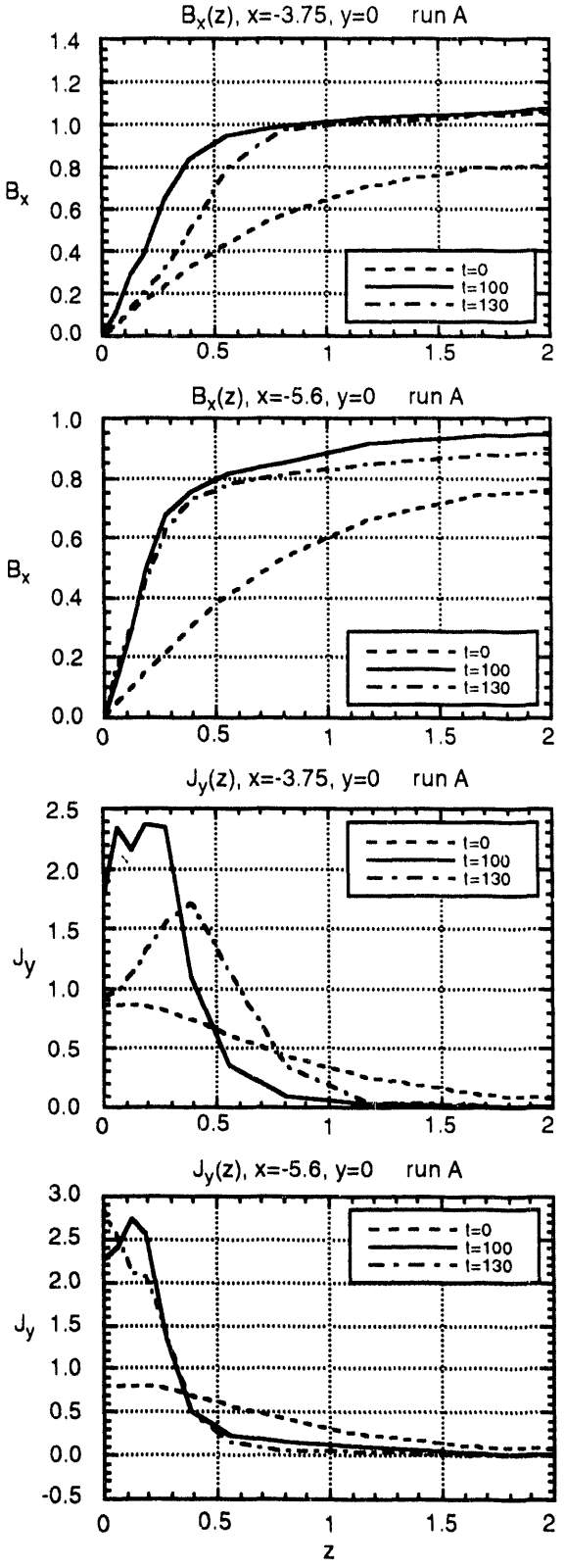

Fig. 7: Variation of B_x and j_y with z for run A at y=0, x=-3.75 and x=-5.6 for three different times, showing the results of the driven current sheet formation (t=100) and the subsequent resistive instability (t=130).

further away from it. The results for run B are quite similar in their spatial variation and therefore not shown here.

A comparison of the two runs with each other and with an earlier run (C), which started from a thick current sheet with constant resistivity [Birn and Hesse, 1991], is provided by the different panels of Fig. 6. The figure shows various quantities as functions of time: (from top to bottom) the maximum current density, the total reconnected flux (integral over negative B_z in the equatorial plane), the maximum tailward and earthward speed, and the total field-aligned current of region 1 signature (toward the Earth in the dawn sector) integrated at the near-Earth boundary.

The top panel of Fig. 6 demonstrates again the driven increase of the current density for runs A and B. Note that, as mentioned earlier, the increase in run A follows an internal time scale of ~50 Alfvén times rather than the external perturbation, which has already subsided after t~20. The onset of reconnection (indicated in panel 2) is followed by a rapid increase in j_y for all three cases, in case A, however, after a brief reduction. Panels 2-4 demonstrate that for the cases with a thin current sheet (A and B) the generation of fast flows closely follows the onset of reconnection, whereas for the thick current sheet the increase in tailward flow already starts before reconnection, but a fast rise of tailward and earthward flow occurs some time later.

Characteristic differences are also shown by the evolution of the (region 1 type) field-aligned current (bottom panel). The breakup of the thick current sheet (C) shows most clearly the spontaneous, that is, nondriven increase in the total region 1 type field-aligned currents ($I_{||}$) after the onset of reconnection, whereas the other cases show only a slight increase of $I_{||}$, in case A after some reduction (similar to the results of Hesse et al., discussed elsewhere in this issue), while case B is still dominated by the driven increase. The reason for the difference in region 1 type currents might simply be the fact that cases A and B were not as evolved as case C when they were terminated. In fact, more recent runs which could be followed for a somewhat longer time showed a more visible increase in $I_{||}$.

Further details of the current "disruption" are shown in Figure 7 for run A; results of run B are quite similar and therefore not shown here. The figure shows B_x and j_y as functions of z similar to Fig. 4, but at two locations further earthward. It demonstrates a complicated behavior of the current density associated with the breakup. Closest to the Earth, at x=-3.75, one can see the reduction of the current density together with a shift to larger z values, but without significant decrease in the total current, measured by the lobe magnetic field. Further tailward, however, at x=-5.6 and x=-7.5 (Fig. 4), the lobe field strength and hence the total current get reduced, while the current density at z=0 remains unchanged at x=-5.6 and even increases at x=-7.5, which is close to the neutral line. In run B the decrease of the lobe field is not as significant, mainly due to the continued driving, but perhaps also to the more restricted effects of localized resistivity.

5. Summary and Conclusions

The dynamic evolution of the magnetotail during growth phase and expansion phase of a substorm has been studied through three-dimensional time-dependent MHD simulations. Starting from a realistic three-dimensional equilibrium model of the tail,

an external electric field with an equatorward inflow was applied at the boundaries, decreasing tailward, flankward, and equatorward. The electric field, which is applied only over a finite period, leads to the formation of a thin current sheet in the near tail, embedded in the wider plasma/current sheet, which becomes diminished in strength. A strong increase in the current density is found for a moderate increase in the lobe magnetic field strength. The current sheet forms on an internal time scale of about 10 minutes if the external change occurs in a shorter time; otherwise the formation follows the external time scale. The driven current sheet formation is accompanied by a 3-4 fold increase in the region 1 type field-aligned currents (toward the Earth on the dawnside, away on the duskside).

A faster, spontaneous current sheet formation occurs when entropy conservation is released in an isobaric model, while the ideal MHD constraint persists. In this case a thin current sheet forms even without external driving on a time scale of about one minute. This may be a suitable model for the late, explosive part of the growth phase [Ohtani et al., 1992].

The transition to the substorm expansive phase was modeled by an increase in anomalous resistivity. In run A this resistivity was applied uniformly after the thin current sheet has formed, while in run B the resistivity was assumed to depend on the current density, requiring a minimum of four times the initial maximum current density to be turned on. The results of both runs are quite similar, except that run B exhibits a more explosive growth; both runs show more rapid changes than the disruption of a wider current sheet (run C), investigated earlier [Birn and Hesse, 1991]. In all cases the violation of ideal MHD leads to the formation of a near-Earth neutral line, fast flows, and plasmoid ejection, together with the dipolarization and current reduction affecting the near tail.

A detailed study of the magnetic field and current changes in the near tail region generally confirm the view that the dipolarization is associated with a current disruption, or rather, reduction of the cross-tail current. However, this is not a local association. The location where the total current gets reduced is typically further tailward than the dipolarization region. Locally we find a rather complicated behavior. Closest to the Earth the current density gets reduced near the neutral sheet but increases further away from it, while the total current does not change significantly. Somewhat further tailward but still earthward of the neutral line, as well as in the vicinity of the neutral line, the current density increases near the neutral sheet but decreases drastically above and below. This decrease is responsible for the decrease in the total current.

The spontaneous increase in region 1 type field-aligned currents $I_{\parallel}$ is not quite as noticable (yet) for the disruption of the thin current sheets as in an earlier simulation of disruption of a wider current sheet (run C), whereas the driven increase in the region 1 type currents is significant. A possible reason for these differences is the fact that runs A and B terminated (for numerical reasons) before the disruption of the thin current sheet could propagate to the thicker plasma/current sheet. Indeed, more recent simulations not reported here, which could be run somewhat longer, showed the increase in $I_{\parallel}$ more clearly. Nevertheless it is remarkable that the behavior of the region 1 type currents may be dominated by the driven effects, while other quantities, such as the maximum flow speeds or electric fields show drastic spontaneous increases. This result demonstrates that the same dynamic process which appears spontaneous from the observation of some particular quantities

might be interpreted as entirely driven from the observation of others. One should therefore apply these terms with caution.

Acknowledgments. This work was supported by the U.S. Department of Energy's Office of Basic Energy Sciences, by NASA's Space Physics Theory Program, and by the Deutsche Forschungsgemeinschaft.

References

Birn, J., Magnetotail equilibrium theory: The general three-dimensional solution, *J. Geophys. Res.*, *92*, 11,101, 1987.

Birn, J., and M. Hesse, The substorm current wedge and field-aligned currents in MHD simulations of magnetotail reconnection, *J. Geophys. Res.*, *96*, 1611, 1991.

Birn, J., K. Schindler, L. Janicke, and M. Hesse, Magnetotail dynamics under isobaric constraints, *J. Geophys. Res.*, in press, 1994.

Erickson, G. M., and M. Heinemann, A mechanism for magnetospheric substorms, in *Substorms 1. Proc. First Int. Conf. on Substorms*, Kiruna, Sweden, 23-27 March 1992, *ESA~SP-335*, p.545, ESA, Noordwijk, The Netherlands, 1992.

Hones, E. W., Jr., T. Pytte, and H. I. West, Associations of geomagnetic activity with plasma sheet thinning and expansion: A statistical study, *J. Geophys. Res.*, *89*, 5471, 1984.

Lui, A. T. Y., C.-L. Chang, A. Mankofsky, H.-K. Wong, and D. Winske, A cross-field current instability for substorm expansions, *J. Geophys. Res.*, *96*, 11,389, 1991.

Lui, A. T. Y., R. E. Lopez, B. J. Anderson, K. Takahashi, L. J. Zanetti, R. W. McEntire, T. A. Potemra, D. M. Klumpar, E. M. Greene, and R. Strangeway, Current disruptions in the near-Earth neutral sheet region, *J. Geophys. Res.*, *97*, 1461, 1992.

McPherron, R. L., A. Nishida, and C. T. Russell, Is near-Earth current sheet thinning the cause of auroral substorm onset?, in *Quantitative Modeling of Magnetosphere-Ionosphere Coupling Processes*, edited by Y. Kamide and R. A. Wolf, p. 252, Kyoto Sangyo University, Kyoto, Japan, 1987.

Mitchell, D. G., D. J. Williams, C. Y. Huang, L. A. Frank, and C. T. Russell, Current carriers in the near-Earth cross-tail current sheet during substorm growth phase, *Geophys. Res. Lett.*, *17*, 583, 1990.

Ohtani, S., K. Takahashi, L. J. Zanetti, T. A. Potemra, R. W. McEntire, and T. Iijima, Initial signatures of magnetic field and energetic particle fluxes at tail reconfiguration: Explosive growth phase, *J. Geophys. Res.*, *97*, 19,311, 1992.

Pulkkinen, T. I., D. N. Baker, D. G. Mitchell, R. L. McPherron, C. Y. Huang, and L. A. Frank, Global and local current sheet thickness estimates during the late growth phase, in *Substorms 1, Proc. First Int. Conf. on Substorms*, Kiruna, Sweden, 23-27 March 1992, *ESA~SP-335*, p.131, ESA, Noordwijk, The Netherlands, 1992.

Sauvaud, J.-A., A. Saint-Marc, J. Dandouras, H. Rème, A. Korth, G. Kremser, and G. K. Parks, A multisatellite study of the plasma sheet dynamics at substorm onset, *Geophys. Res. Lett.*, *11*, 500, 1984.

Schindler, K., A theory of the substorm mechanism, *J. Geophys. Res.*, *79*, 2803, 1974.

Schindler, K., and J. Birn, On the cause of thin current sheets in the near-Earth magnetotail and their possible significance for magnetospheric substorms, *J. Geophys. Res.*, *98*, 15,477, 1993.

Sergeev, V. A., D. G. Mitchell, C. T. Russell, and D. J. Williams, Structure of the tail plasma/current sheet at 11 R_E and its changes in the course of a substorm, *J. Geophys. Res.*, *98*, 17,345, 1993.

DATE

FILMED

6/15/94

END